



## DESIGN AN UNCERTAIN MODEL FOR THE STUBBED GROUND PLANE BY INCREASING THE BANDWIDTH OF THE MONOPOLE ANTENNA

D. JASMINE DAVID\*, K. RAMALAKSHMI†, M. SELVARATHI‡, T.JEMIMA JEBASEELI§, P. SURESH¶, AND P.DHIVYA ||

**Abstract.** Uncertainty is stated as the indication of the quality of the calibration certificate. When uncertainties occurred in a stubbed ground plane, it affects the performance of every source. Hence, a thorough analysis of uncertainties on a monopole antenna is required. The proposed research work is to focus on designing a planar monopole antenna to improve the bandwidth with minimal changes on the ground plane mainly for medical applications and to reduce the uncertainty. The narrowband antenna on the ground plane is redesigned to boost up the gain and broadens the monopole antenna's bandwidth impedance. Then the ground plane is integrated with the rectangular plate. As a result the bandwidth is 42.5 GHz ahead.

**Key words:** Bandwidth; monopole antenna; stubbed ground plane; uncertainty, wireless communication.

**AMS subject classifications.** 68M14, 78A50

**1. Introduction.** There is a lot of interest in developing on-body monitoring devices. Now, people are more aware of and accepting of healthcare technology. A Body Area Network (BAN) is the foundational mechanism for tracking human health concerns. [1]. BANs apply to both the commercial and healthcare sectors. Despite their different applications, the criteria of devices grouped around the BAN are demanding, including miniaturization, ultra-light weightless, discreetness, cost, self-sustainability, and safety. While retaining the intended functioning, the gadgets must interfere with human mobility as little as possible [2]. These on-body devices are intended to monitor human activity and collect crucial physiological and clinical signals to monitor the health of the aged, disabled, and any other sick patients, as well as a tracking system.

**2. Literature Review.** Wideband systems have non-ionizing radiation qualities; higher resolution, and great penetration capacity, wideband systems have been effectively adopted into healthcare [3]. It also appears to be tolerant of modulation devices due to its very low transmit power to high-frequency range [4]. A wideband antenna is a pass filter and sends small pulses rather than a continuous carrier wave; distortion and wave spreading are also reduced, resulting in more efficient transmission. A variety of antennas for uncertain approaches have been proposed. Some of them are simple modifications to ordinary antennas that have been used for decades [5]. The modified planar monopole antenna is one such uncertain antenna that has demonstrated potential wideband performance. Planar monopole antennas have several benefits due to their simple design and omnidirectional emission pattern [6-7]. The ground plane is embedded with microstrip lines, and readily integrated with microwave circuitry. Boosting the bandwidth, many ways to alter monopole antennas have been tried [8-12]. Some of these include dielectric resonators, annular slots, inverse T of ground planes, simple bevel design, feature smoothing, shorting pins, fractal feature creation, open slot insertion, spurious feature integration, use of substrates of varying thicknesses, and truncated ground planes [13-15].

Impedance matching is performed on a small monopole antenna by inserting a stub on the radiating section of the antenna or on its ground plane. It is less difficult to implement. Different sorts of uncertain

---

\*This work was supported by Karunya Institute of Technology and Sciences.

Assistant Professor, ECE, Karunya Institute of Technology and Sciences, Coimbatore, India ([jasmine@karunya.edu](mailto:jasmine@karunya.edu))

† Associate Professor, CSE, Alliance University, Bangalore, India ([ramalakshmivenkatesan@gmail.com](mailto:ramalakshmivenkatesan@gmail.com))

‡ Assistant Professor, Mathematics, Karunya Institute of Technology and Sciences, Coimbatore, India ([selvarathi@karunya.edu](mailto:selvarathi@karunya.edu))

§ Associate Professor, CSE, Karunya Institute of Technology and Sciences, Coimbatore, India ([jemima\\_jeba@karunya.edu](mailto:jemima_jeba@karunya.edu))

¶ Assistant Professor, AI&DS, M. Kumarasamy College of Engineering, Karur, India ([psuresh82@gmail.com](mailto:psuresh82@gmail.com))

|| Assistant Professor, CSBS, M. Kumarasamy College of Engineering, Karur, India ([dhivyaainfo@gmail.com](mailto:dhivyaainfo@gmail.com))

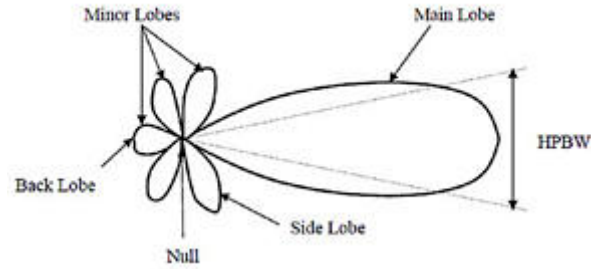


Fig. 3.1: Radiation pattern of general directional antenna.

stub structures have different outcomes [16-18]. Its primary application is to improve bandwidth and radiation characteristics. In this article, we have modified a small circular unbalanced antenna to provide an extremely broadband body health monitoring system. The radiating component has spherical and circular slots and 50 microstrip lines. The modified partial ground plane includes a smaller rectangular area that acts as an efficient impedance matching device to increase bandwidth and reduce uncertainty. It is made up of Kepton material. The stray or edge capacitance will be impacted by the microstrip thickness. Specifically, the stray capacitance of the conductor increases as conductor thickness increases.

**3. Methodology.** In a wireless communication system, the antenna is a vital component. A well-designed antenna can minimize system requirements and uncertainty while boosting overall performance.

**3.1. Radiation Pattern.** The radiation of the antenna depicts the radiation qualities in the far-field as a function of spatial coordinates defined by the elevation angle  $\theta$  and the azimuth angle  $\phi$ . This is a graph of the radiated antenna's power.

Take the anisotropic antenna as an example. An isotropic antenna radiates in the same direction in all directions. If an isotropic antenna radiates total power  $P$ , the power is spread with radius  $r$ , and density  $S$  is given in the following equation.

$$s = \frac{p}{area} = \frac{p}{4\pi r^2} \quad (3.1)$$

$$U_i = sr^2 = \frac{p}{4\pi r^2} \quad (3.2)$$

$U_i$  denotes the isotropic antenna's radiation intensity.

The directional antenna is a more practical form of dissipating more power in one direction and less power in another. An omnidirectional antenna has a consistent radiation in E-plane but changes in H-plane. The description of the different phases of Figure 3.1 is as follows.

- PBW: The angle is determined not entirely by the half-power.
- Main Lobe: It's the largest radial direction of the lobe.
- Minor Lobe: All minor lobes except major lobes are classified as minor lobes. The minor lobes emit radiation in an unfavorable direction.
- Back Lobe: It is the exact opposite of the minor lobe.
- Side Lobes: These are sidelobes separated by zero from the main lobe. Minor lobes are the most prominent of the minor lobes.
- Sidelobes are not desirable in most wireless systems. Sidelobes are the largest of the sidelobes. Sidelobes are not desirable in most wireless systems. Therefore, a good antenna design should prevent small lobes.

**3.2. Directivity.** The proportion of the force of radiation transmitted by the uncertain antenna in a ground plane to the normal power of radiation discharged by the receiving wire every which way is characterized

as the receiving wire's directivity.

$$s = \frac{U}{U_i} = \frac{4\pi U}{P} \quad (3.3)$$

where  $D$  denotes antenna's directivity and  $U$  denotes antenna's radiation intensity. The radiation intensity of an isotropic source is denoted by  $U_i$ .

The complete power transmitted is indicated by  $P$ . The bearing of the directivity isn't given all of the time. In this uncertain situation, the highest directivity is implied by the direction of maximum radiation intensity:

$$D_{max} = \frac{U_{max}}{U_i} = \frac{4\pi U_{max}}{P} \quad (3.4)$$

The greatest radiation force is meant by  $U_{max}$ . Since it is the proportion of two radiation forces, directivity is a dimensionless amount. As a result, it is often expressed in decibels (dBi). An antenna's radiation pattern may be easily utilized to calculate its directivity.

**3.3. Input Impedance.** The impedance presented by a receiving wire at its terminals is characterized as the voltage to flow proportion at the sets of terminals or the proportion of the pertinent parts at a given position. As a result, the impedance of the radio wire might be composed as:

$$Z_{in} = R_{in} + jX_{in} Z_s = R_s + jX_s \quad (3.5)$$

The imaginary part  $X$  is the information impedance addresses where the power is put away near the radiation field. The resistive impedance at input  $R$  is involved two segments sections:  $R_i$  is the radiation obstruction and  $R_L$  is the resistance loss. The power-related to the radiation opposition addresses the genuine power transmitted by the radio wire, while the uncertain power squandered in the misfortune obstruction is lost as hotness in the receiving wire because of dielectric or conductive misfortunes.

**3.4. Voltage Standing Wave Ratio (VSWR).** The impedance mismatch between the transmitter and the antenna is assessed by VSWR. Higher the VSWR, then there will be a greater disparity. VSWR compares to an ideal pair. Because of the way that most antenna design is intended for this uncertain impedance, a satisfactory receiving antenna configuration ought to have an information impedance of  $50 \Omega$  or  $75 \Omega$ . A VSWR of 1:1 denotes an ideal match.

**3.5. Return Loss.** Return Loss concludes how much power is lost to the load. At the point when the transmitter and antenna impedance don't coordinate, hence it reflects the waves. This result leads to the arrangement of standing waves, as portrayed in the previous section.

$R_L$  metric reflects how well the transmitter and antenna have been matched.

The expression for  $R_L$  is given in equation (3.6) to ensure that the transmitter and antenna are perfectly matched.

$$R_L = -20 \log_{10} \Gamma \quad (3.6)$$

$\Gamma = 0$  and  $R_L = \infty$  implying that no power is reflected.

**3.6. Antenna Efficiency.** The antenna efficiency is an action that thinks about how much loss is at the receiving wire's terminals as well as inside the antenna's design. These losses are caused by,

- Reflections are induced by an uncertain antenna-to-transmitter mismatch.
- I2R is the loss due to conduction.

As a consequence, the efficiency of the antenna's function is expressed as follows:

$$e_t = e_r e_c e_d \quad (3.7)$$

where  $e_t$  stands for total antenna efficiency.  $e_r = (1 - \Gamma^2)$  efficiency of reflection.

The conduction efficiency is denoted by  $e_c$ .  $e_c$  and  $e_d$  are combined to generate efficiency  $e_{cd}$ . This is expressed as follows:

$$e_{cd} = e_c e_d = \frac{R_r}{R_r + R_L} \quad (3.8)$$

where  $e_{cd}$  is the ratio of power sent to  $R_r$  to  $R_r$  and  $R_L$  is known as antenna radiation efficiency.

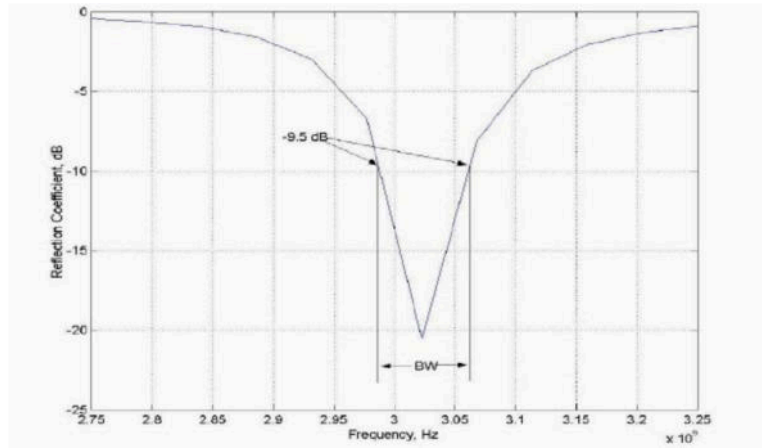


Fig. 3.2: Bandwidth measurement

**3.7. Antenna Gain.** Antenna gain is a quantity that strongly connected the directivity of the antenna. The amount of energy that an antenna concentrates in one direction over other emission directions is referred to as directivity. As a result, if the antenna is efficient, the directivity equals the antenna gain. The gain is generally connected to the primary flap and provided toward most elevated radiation is portrayed as follows:

$$G(\theta, \phi) = e_{cd}(\theta, \phi) \quad (3.9)$$

**3.8. Bandwidth.** The data transmission and the bandwidth are characterized as the usable frequencies comparable to some predetermined standard. The transfer speed of a broadband antenna is characterized as the proportion of satisfactory higher to bring down frequencies. The transmission capacity is characterized as the proportion of fluctuation across center frequency. It is defined as follows:

$$BW_{broadband} = \frac{f_H}{f_L} \quad (3.10)$$

$$BW_{narrowband}(\%) = \frac{(f_H - f_L)}{f_c} \quad (3.11)$$

where  $f_H$  denotes the maximum cut-off frequency.  $f_L$  is the lower cut-off frequency, and  $f_c$  is the center frequency. If  $f_c$  is the center frequency. If  $\frac{f_H}{f_L} = 2$ , an antenna is considered to be broadband.

Measuring an antenna's VSWR is one approach to determine how effectively it operates over the desired frequency range. Figure 3.2 depicts bandwidth measurement.

**3.9. Beam Width.** The bandwidth of the antenna is the shaft width. After determining the radiation intensity, the spots on each side of the peak intensity are identified. The half-power beam width is 3dB. Assume that the bulk of the radiated power is not divided into side lobes. Thus the directive gain is inversely proportional to the beam width. As the beam width decreases, the directive gain decrease as well.

The matching slots might still be employed on here just to alter the compatibility even if matching slots in microstrip patch are half-wave resonance. Similar to a wire mesh monopole, the monopole's bandwidth is enhanced because it is circular. The bandwidth of thick monopoles is greater than that of thin monopoles. The matching and the bandwidth are both affected by the curvature of the ground; typically, the match defines the bandwidth, thus modifying one affects another. This is a microstrip-fed monopole with an extended ground instead of a flat ground that runs perpendicular to the monopole; it is not a microstrip patches with a partial ground. The stray or edge capacitance will be impacted by the microstrip thickness. Specifically, the stray capacitance of the conductor increases as conductor thickness increases.

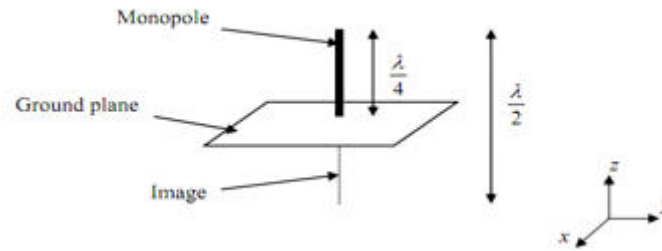


Fig. 4.1: Monopole antenna structure.

**3.10. Side Lobes.** There is none of the antenna emit all of their energy in a single chosen direction. Some of it will certainly be radiated in other ways. The peaks are known as side lobes, and they are generally described in decibels down from the main lobe.

**3.11. Nulls.** An invalid zone in a receiving antenna radiation design is viable with t minimal transmitted power. An invalid as often as possible has a smaller directivity point than the essential beam. Subsequently, the null is useful for an assortment of reasons including remembering the concealment of interfering signs for a specific direction.

**3.12. Radiation Resistance.** Resistance to Radiation is described as a fake or hypothetical resistance that dissipates the same amount of power as the radiated power.

$$R_r = \frac{\text{Power Radiated}}{I_r^2 m s} \quad (3.12)$$

**3.13. Radiation Intensity.** The power emitted in a specific direction per unit solid angle is known as radiation intensity.

$$RI = \frac{r^2 E^2}{\eta_0} = r^2 P \frac{\text{Watts}}{\text{unit solid angle}} \quad (3.13)$$

Here  $\eta_0$  = intrinsic impedance,  $r$  = radius of the sphere (meter)  $P$  = power radiated instantaneously,  $E$  = Electric Field Strength (V/m).

**4. Monopole Antenna Design.** The monopole antenna is the consequence of utilizing the structure hypothesis on a dipole [19-20]. Assuming a directing plane is set under a solitary component of length  $L/2$  conveying a current, the component and its picture act indistinguishably from a dipole of length  $L$ , with the provision that radiation happens just over the uncertain ground plane, as portrayed by Saunders. Figure 4.1 tells the best way to construct a monopole antenna.

The top ground raises the line's capacitance, decreases its impedance, and perhaps most likely modifies the dielectric characteristic constant and the value of velocity. If the vias were too near to the edge, it could increase capacitance and interfere with other processes. They would cause a cyclic disturbance in the capacitance, perhaps lowering the maximum working frequencies. This will not occur if the vias are sufficiently distant from the edge. To add frequency sweep, the following procedures are required. First select the menu item HFSS, Analysis Setup, Add Sweep. Then, select Solution Setup: Setup1. Then, Edit Sweep Window with Sweep Type as Fast and Frequency Setup Type as Linear Count. Finally, Give Start and stop frequency as 5 GHz and 10 GHz in terms of Count as 500.

The antenna's directivity is doubled and its radiation resistance is half that of a dipole. A quarter-wave monopole can have the same properties as half-wave dipoles. Monopoles are astoundingly useful in convenient antennas, where the uncertain coordinating plane might be the body of the vehicle or the phone shell. The quarter frequency monopole regularly has an increase of 2-6dB and a data transmission of around 10%. It has

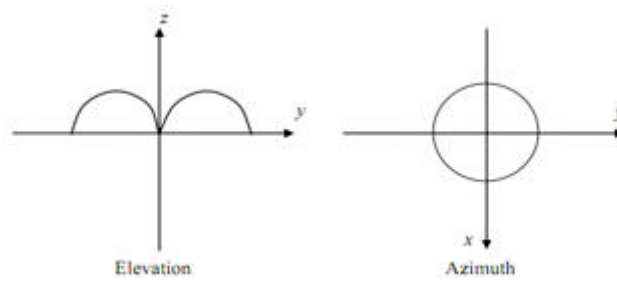


Fig. 4.2: The monopole antenna's radiation pattern.

Table 4.1: Particulars of design

PARAMETER	DIMENSIONS (in mm)	
	LENGTH	WIDTH
SUBSTRATE (FR4 epoxy)	40	60
GROUND	40	22
STRIP LINE	20	2
GAP	2	22

a 36.5 radiation resistance and directivity of 3.28. (5.16dB). Figure 4.2 portrays the radiation example of a monopole. Table 4.1 portrays the details of the design.

**5. Compact Antennas Feed Analysis.** The simplest extraction approach is a microstrip line feed, which has the benefit of feeding in the same plane as the radiating monopole. When integrating the big arrays of feeding network f, this way of simply attaching a 'U' patch at the edge is quite convenient. However, the patch's erroneous radiation causes issues. Prior knowledge of the feed point position is essential for impedance matching in this form of stimulation. Figure 5.1 depicts a microstrip line fed rectangular patch.

**6. Experimental Results and Discussions.** The High-performance Full-wave Electromagnetic System (HFES) is an inconsistent 3D volumetric model that uninvolved gadgets with the Microsoft Windows graphical interface. It incorporates representation, strong demonstration, and mechanization in a simple to learn environment to generate results for 3D-EM issues.

Ansoft spearheaded the utilization of the Finite Element Method (FEM) to electromagnetic demonstrating by including innovations like unrelated vector limited components, versatile lattice, and Adaptive Lanczos-Pade Sweep (ALPS). HFSS keeps on driving the market today with the developments like Modes-to Nodes and Full Wave Spice.

Ansoft HFSS has advanced over time because of client and industry input. It is the business standard for high-efficiency and virtual prototyping. As a result, the design is adjusted and the stub is integrated as shown in Figure 6.1 which results in the same reflection coefficient. The VSWR plot in Figure 6.1 shows the obtained UWB. The recurrence goes from 3.29 to 9.33 GHz. The recurrence band for UWB is 3.1 to 10.6 GHz.

The connectors used here are Coax, SFP/XFP, Backplane Transitions. Dielectric constant, bulk conductance, and loss tangent are employed in the battery's HFSS simulation. A reflector must be fixed quarter wavelengths distant from the origin for it to operate. As a result, waves reflected from the ground plane are in sync with and overlaying the waves being created. The reflector is quite near to the patches in the instance of a radiating patch. The waves will not be in phase if it is near to the patch.

A VSWR of 2 represents 11% of the reflected power. As demonstrated in Figure 6.2, a reflected power of 0 dB; where all of the power is reflected, but a reflected value of -10 dB shows that only 10% of the power is

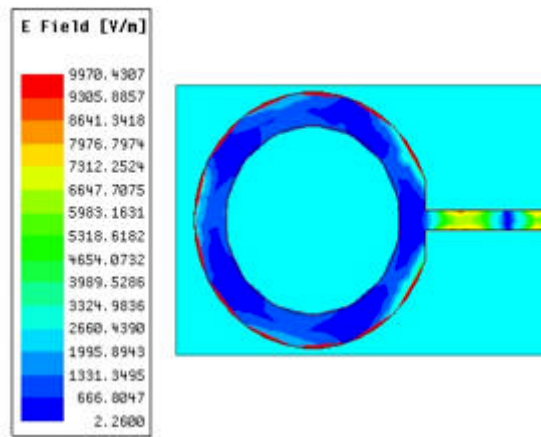


Fig. 5.1: A microstrip line feeds a rectangular patch.

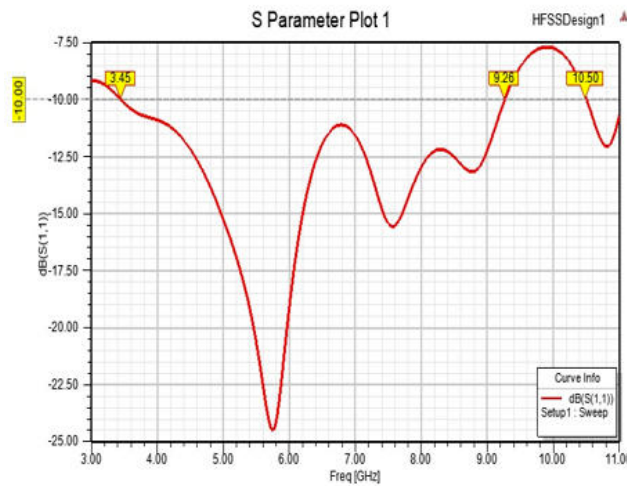


Fig. 6.1: Reflection coefficients are depicted graphically.

reflected. The VSWR would be infinite if 100% of the power was reflected.

The thinner the surface, the greater the loss factor due to increased leak of current density, and hence performance suffers significantly. Furthermore, a narrow track causes increased line impedance, which leads to loss and, as a consequence, a drop in efficiency.

Figure 6.3 depicts the current distributions at the microstrip patch. The passage of current across the ground plane is seen in Figure 6.4. Figure 6.5 shows the monopole antenna surface current: Surface current at 3.1 GHz, 5.7 GHz, 8.0 GHz, and 10.6 GHz (A-D).

It is observed that the dielectric substrate’s thickness is quite thin; as a result, the height-dependent field fluctuation will be constant. When the electric field is normal to the patch’s surface, the fringing effect fields at the patch’s borders are similarly minimal. Five conformal antenna components are used to create the first antenna array, which yields a consistent gain of about 12 dBi with little scan loss over a wide range of scan angles. The antenna’s electrical height is connected to crucial antenna properties such as gain, beam width, reflection coefficient, efficiencies, and so on.

The patch antenna has a resonant frequency. The patch and the ground create a low-impedance microstrip

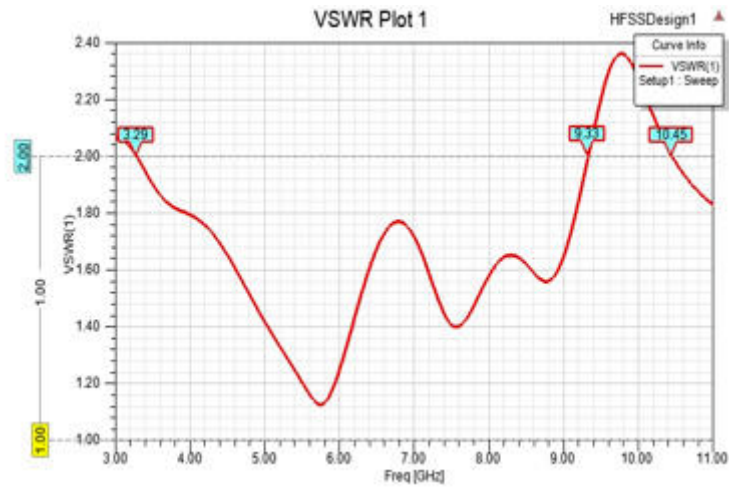


Fig. 6.2: VSWR Plot.

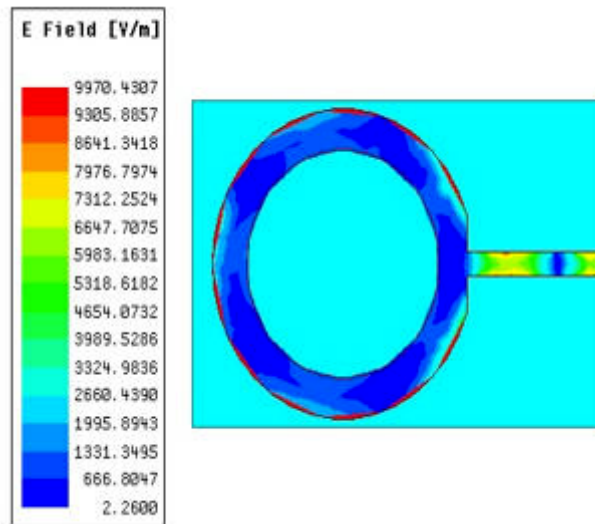


Fig. 6.3: Distributions of current at the microstrip patch.

half-wave resonator, and the fields are mostly in the dielectric underneath the patch. Because the wavelengths in the dielectric are shorter, the length of the patches must be smaller than half a wavelength in the atmosphere. The resistance of the resonator is determined by the size of the patches and the dielectric. Therefore for the same resistance, the patch must be narrower for large dielectric constants, or the dielectric must be thicker.

Table 6.1 shows the obtained values of different performance parameters of the proposed antenna model.

The obtained results of Peak Gain = 2.374932, Peak Realised Gain = 2.367537, and Peak System Gain=2.367537.

**7. Conclusion.** A monopole broadband antenna is proposed in this plan for enlarging the data transfer capacity. A partial ground plane change builds the data transmission from 3 GHz to 37.26 GHz by 170%. Accordingly, the proposed system is accomplished the UWB at frequencies to 10.6 GHz. The antenna properties

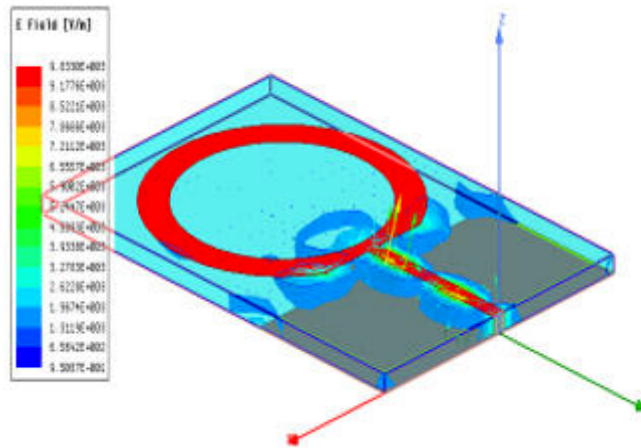


Fig. 6.4: Flow of current through the ground plane.

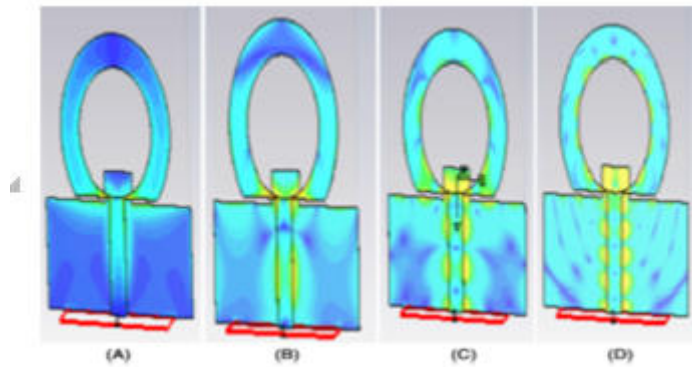


Fig. 6.5: Monopole antenna surface current at 3.1 GHz, 5.7 GHz, 8.0 GHz, and 10.6 GHz (A-D).

Table 6.1: Performance Metrics for the frequency with 5.76 GHz.

QUANTITY	VALUE
Max U	188.398178 mW/sr
Peak Directivity	2.693408
Radiated Power	879.011566 mW
Accepted Power	996.886391 mW
Incident Power	1.000000 W
Radiation Efficiency	88 %
Front to Back Ratio	9.051799
Decay Factor	0.000000
System Power	1.000000 W

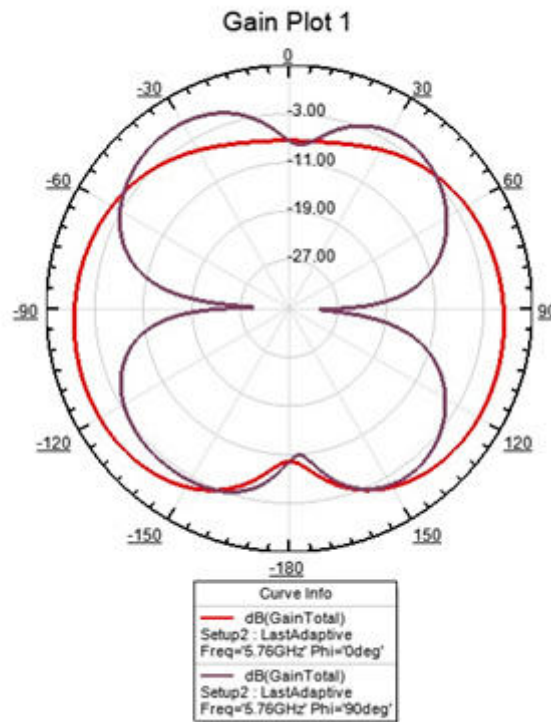


Fig. 6.6: The obtained gain plot.

are being tried tentatively, and it has been found that the antenna is a brilliant competitor for profoundly wideband applications. This plan explores the possibility of bandwidth improvement on an uncertain stubbed ground plane by the circumstance of a stub on the edge of the partial ground plane as an impedance matching instrument for the antenna. Since the antenna is being proposed for use in clinical applications, it should be analyzed to comprehend the impact of human body proximity, which will be accounted for in future correspondence.

#### REFERENCES

- [1] IEEE 802.15 Working Group for WPAN. 2000.
- [2] Soh PJ, Vandenbosch GAE, Ooi SL, Husna MRN. Wearable dualband Sierpinski fractal PIFA using conductive fabric. *Electron Lett.* 2011; 47(6):365-367.
- [3] Soh PJ, Boyes SJ, Vandenbosch GAE, Huang Y, Ooi SL. On-body characterization of a dual-band, all-textile PIFA. *Prog Electromagn Res.* 2012; 129:517-539.
- [4] Iwasaki H. A circularly polarized small-size microstrip antenna with a cross slot. *IEEE Trans Antennas Propag.* 1996;44(10):1399-1401.
- [5] Lilja J, Salonen P, Kaija T, de Maagt P. Design and manufacturing of robust textile antennas for harsh environments. *IEEE Trans Antennas Propag.* 2012; 60(9):4130-4140.
- [6] Park S, Jayaraman S. Enhancing the quality of life through wearable technology. *IEEE Eng Med Biol Mag.* 2003; 22(3):41-48.
- [7] Declercq F, Rogier H. Active integrated wearable textile antenna with optimized noise characteristics. *IEEE Trans Antennas Propag.* 2010; 50(9): 3050-3054.
- [8] Lee HJ, Ford KL, Langley RJ. Switchable on/off body communication at 2.45 GHz using textile microstrip patch antenna on stripline. *Electron Lett.* 2012; 48(5):254-256.
- [9] Axisa F, Schmitt P, Gehin C, Delhomme G, McAdams E, Dittmar A. Flexible technologies and smart clothing for citizen medicine, home healthcare, and disease prevention. *IEEE Trans Inf Technol. Biomed.* 2005; 9(3):325-336.

- [10] Yang LQ, Giannakis GB. Ultra-wideband communications: an idea whose time has come. *IEEE Signal Process Mag.* 2004; 21: 26-54.
- [11] Powell J, Chandrakasan A. Spiral slot patch antenna and circular disc monopole antenna for 3.1–10.6 GHz ultra-wideband communication, *Proc 2004 ISAP*, Sendai, Japan, 2004: 85–88.
- [12] Ammann MJ, Chen ZN. Wideband monopole antennas for multiband wireless systems. *IEEE Antennas Propag Mag.* 2003;45(2):146-150.
- [13] Liang J, Chiau CC, Chen X, Parini CG. Analysis and design of UWB disc monopole antennas. 2004 IEE Seminar on Ultra Wideband Communications Technologies and System Design, 2004: 103-106.
- [14] Kalyan Mondal, Axial Ratio (AR) and Impedance Bandwidth (IBW) enhancement of Circular Polarized (CP) monopole antenna, *AEU - International Journal of Electronics and Communications*, Volume 134, 2021.
- [15] Narinder Sharma, Sumeet Singh Bhatia, Ultra-wideband fractal antenna using rhombus shaped patch with stub loaded defected ground plane: Design and measurement, *AEU - International Journal of Electronics and Communications*, Volume 131, 2021.
- [16] Hussein Alsariera, Zahriladha Zakaria, Azmi bin Awang Md Isa, New broadband L-shaped CPW-fed circularly polarized monopole antenna with asymmetric modified ground plane and a couple series-aligning inverted L-shaped strip, *AEU - International Journal of Electronics and Communications*, Volume 118, 2020.
- [17] Utsab Banerjee, Anirban Karmakar, Anuradha Saha, Piyali Chakraborty, A CPW-fed compact monopole antenna with defected ground structure and modified parasitic hilbert strip having wideband circular polarization, *AEU - International Journal of Electronics and Communications*, Volume 110, 2019.
- [18] Rohit Gurjar, Dharmendra K. Upadhyay, Binod K. Kanaujia, Amit Kumar, A compact modified sierpinski carpet fractal UWB MIMO antenna with square-shaped funnel-like ground stub, *AEU - International Journal of Electronics and Communications*, Volume 117, 2020.
- [19] Xiaohua Tan, Weimin Wang, Yongle Wu, Yuanan Liu, Ahmed A. Kishk, Heng Wang, Enhancing isolation and bandwidth in planar monopole multiple antennas using thin inductive line resonator, *AEU - International Journal of Electronics and Communications*, Volume 117, 2020.
- [20] Rohit Mathur, Santanu Dwari, Compact CPW-Fed ultrawideband MIMO antenna using hexagonal ring monopole antenna elements, *AEU - International Journal of Electronics and Communications*, Volume 93, Pages 1-6, 2018.

*Edited by:* Vinoth Kumar

*Received:* Aug 13, 2022

*Accepted:* Nov 18, 2022